Reprinted from

Réimpression du

574

Canadian Geotechnical Journal

Revue canadienne de géotechnique

Strength of tree roots and landslides on Prince of Wales Island, Alaska

Tien H. Wu, William P. McKinnell III, and Douglas N. Swanston

Volume 16 · Number/numéro 1 · 1979
Pages 19–33

National Research Council Canada
Conseil national de recherches Canada

Strength of tree roots and landslides on Prince of Wales Island, Alaska

TIEN H. WU
Department of Civil Engineering, The Ohio State University, Columbus, OH 43210, U.S.A.

AND

WILLIAM P. MCKINNELL III
Chen and Associates, 965 Zuni St., Denver, CO 80223, U.S.A.

AND

DOUGLAS N. SWANSTON
Forest Sciences Laboratory, Pacific Northwest Forest and Range Experiment Station, USDA Forest Service, Corvallis, OR 97331, U.S.A.

Received February 15, 1978

Accepted September 13, 1978

The stability of slopes before and after removal of forest cover was investigated. Porewater pressures and shear strengths were measured and the soil properties were determined by laboratory and *in situ* tests. A model of the soil–root system was developed to evaluate the contribution of tree roots to shear strength. The computed safety factors are in general agreement with observed behaviors of the slopes. Decay of tree roots subsequent to logging was found to cause a reduction in the shear strength of the soil–root system.

La stabilité des pentes avant et après déboisement a été étudiée. Les pressions interstitielles et les résistances au cisaillement ont été mesurées et les propriétés géotechniques ont été déterminées par essais en laboratoire et *in situ*. On a développé un modèle du système sol–racines pour évaluer la contribution des racines d'arbres à la résistance au cisaillement. Les facteurs de sécurité calculés sont généralement en accord avec le comportement observé des pentes. On a trouvé que la décomposition des racines après le déboisement produit une réduction de la résistance au cisaillement du système sol–racines.

[Traduit par la revue]

Can. Geotech. J., 16, 19–33 (1979)

Introduction

Landslides that involve the shallow surface soils have been observed to be an important form of mass wastage on steep hillsides of southeastern Alaska (Bishop and Stevens 1964). The landslides have been classified as debris avalanches (Swanston 1969) using the classification system of Varnes (1958). The typical landslide begins as a rotational slip located in the upper part of a slope, usually at the head of a small gully or drainage depression. The extent of the slip may cover an area no greater than 12 m by 12 m. The depth of the slip surface is about the same as the depth of the weathered soil, which usually ranges from 1–1.5 m. As the sliding mass moves downhill, additional soil in the path of the movement is disturbed and carried along. Because of the high water content, the movement during the later stages has the characteristics of viscous flow. The result is a long scar that begins at the location of the initial slide and extends almost all the way to the base of the slope. Such landslides remove valuable top soil, cause siltation of streams, present hazards in inhabited areas, and represent a serious problem in geotechnical engineering.

While slides occur in forested areas, it has also been observed that the frequency of slides is much greater on slopes where the forest has been removed by clear-cutting (Bishop and Stevens 1964). Extensive logging by clear-cutting has been carried out on Prince of Wales Island in the vicinity of Hollis and Thorne Bay (Fig. 1). The Maybeso Valley near Hollis (Fig. 2) was logged mostly between 1954 and 1960. Numerous landslides have occurred on the slopes of the valley with the majority of the slides taking place around 1961. Afterwards, isolated slides occurred occasionally. Logging in the Thorne Bay area is more recent. Numerous slides have occurred on several valley slopes after logging. Most of the slides occurred during the autumn rain season. To study the effect of clear-cutting on stability, porewater pressures and creep rates were measured at several sites near Hollis from 1964 to 1966 (Swanston 1967, 1970; Barr and Swanston 1970). Additional field measurements were carried out from 1972 through 1975 at sites near

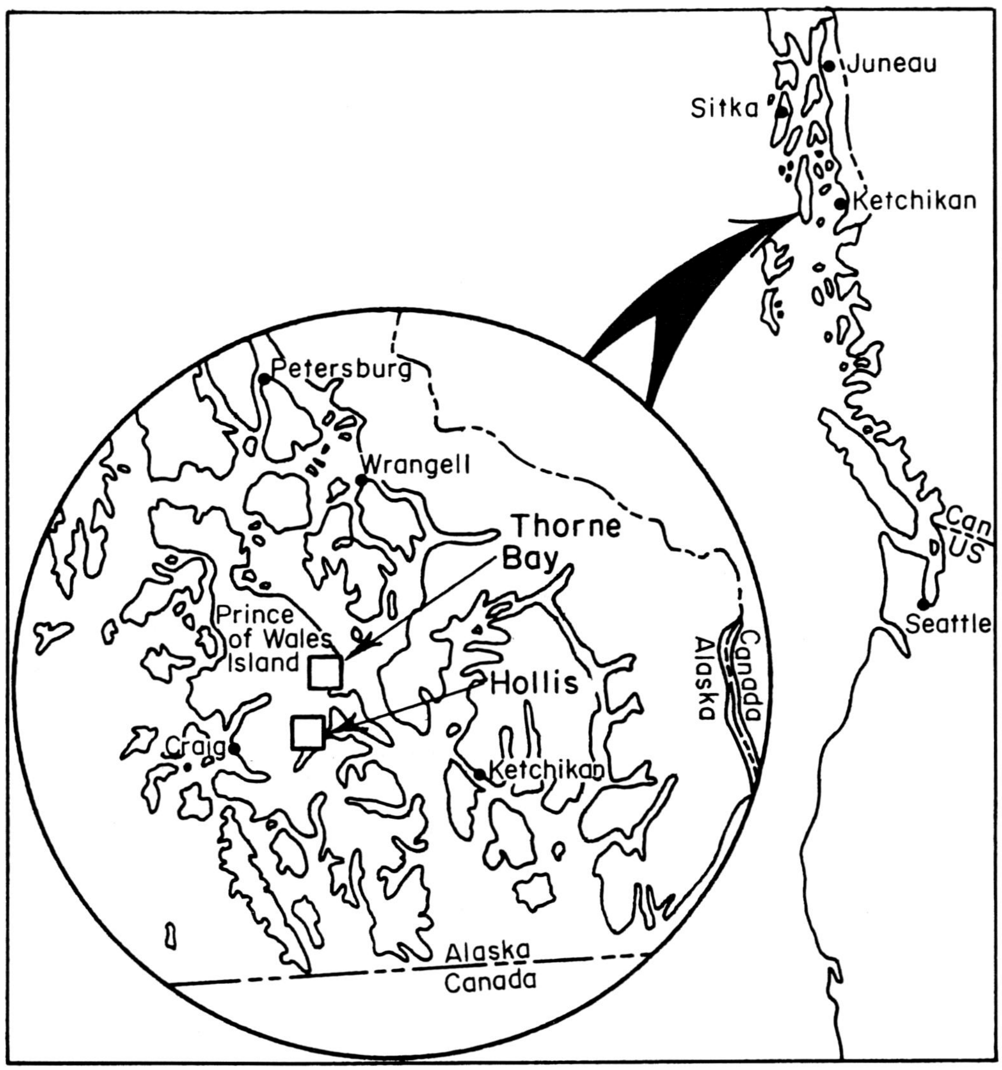

FIG. 1. Location of Hollis and Thorne Bay.

Hollis and near Thorne Bay. This was accompanied by laboratory investigations of soil strength and the contribution of tree roots to shear strength. Stability analyses were made with the data on pore pressure and strength for a number of slopes. The results of these studies are summarized in this paper.

Description of Sites

Area A, located in Maybeso Valley (Fig. 2), includes a portion of the virgin forest and an area logged from 1955 to 1958. The logged area is representative of the regrowth after clear-cutting. In the autumn of 1961 many landslides occurred in the cutover area and these were the subject of the investigations by Swanston (1967, 1970) and Barr and Swanston (1970). This area was given detailed attention because it provides the opportunity to compare the behavior of forested slopes with that of logged slopes. The results of the earlier studies also provide the opportunity to evaluate the effect of regrowth on slope behavior.

A detailed map of area A is shown in Fig. 3. The site conditions are represented by four sections. Section 1 (Fig. 4) passes through a slide scar and is representative of the slides on logged slopes. This is also the area where Swanston (1967, 1970) made his measurements. Outside of the slide scar there is presently a dense regrowth of Sitka spruce, the average height of which is estimated to be about 6 m. Section 2 (Fig. 5) passes through a part of the forest that shows signs of extensive movement. The uneven

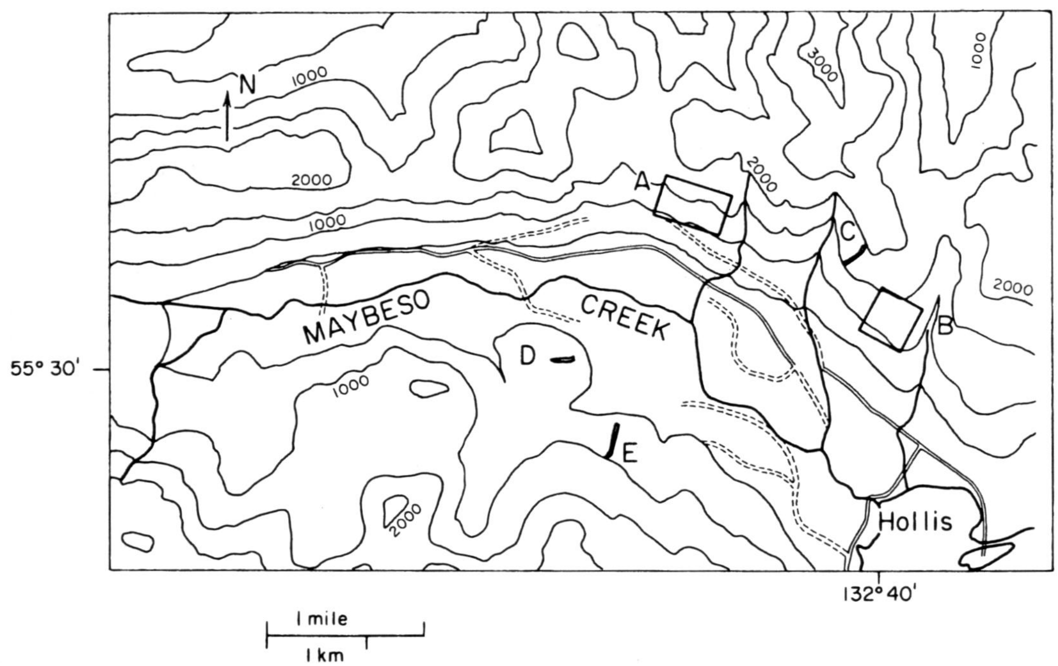

FIG. 2. Map of Hollis area; contour interval = 500 ft (1 ft = 0.3 m).

surface of the ground is the result of many small slides. The movements are concentrated in the steepest part of the slope where the slope angle is about 50°. The soil profile, as seen in test pits excavated in this area (P1, P2, P3), shows only a thin layer of soil. The displaced soil has accumulated on the flatter slope immediately below. Test pit P7 passes through a gray clay layer at a depth of 1 m (40 in.). Below this layer we see the weathered soil or B horizon that has been buried by the slide material. In our interpretation, the gray clay layer was formed as the sliding mass moved over the original ground surface. In general, where the slopes are around 40° or more, small slides have occurred in areas with no trees. Such a slide has occurred along section 3. Soil masses with trees undergo slips if they are undermined by erosion and slips on the downhill side. In contrast to slides on logged slopes, these slides can move only through distances of a few feet before the slide mass is stopped by the larger trees (Fig. 6).

Section 4 (Fig. 7) is representative of the condition in the forest west of the small creek indicated by J in Fig. 3. This slope apparently has been stable for many years as there are no signs of recent movements. The weathered zone in test pit P9 is about 1.5 m thick.

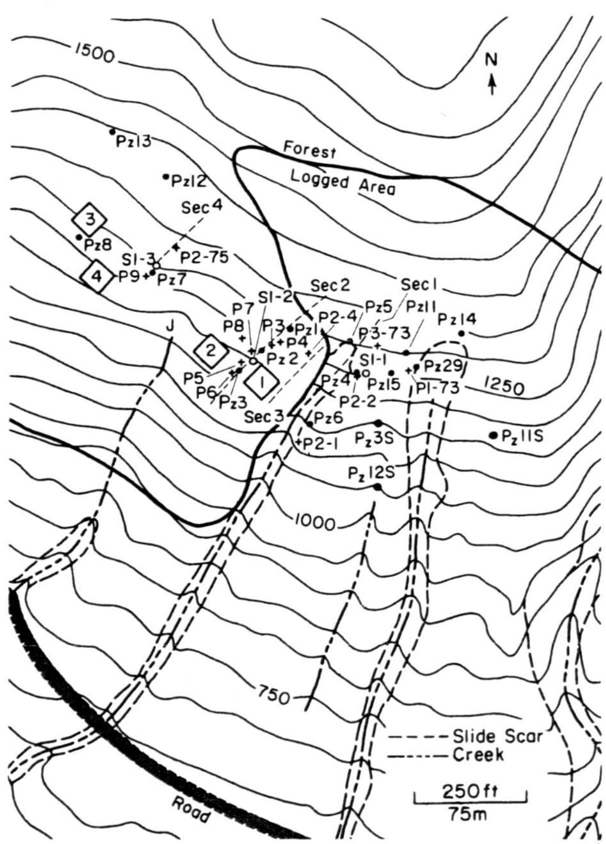

FIG. 3. Map of area A. ●Pz = piezometer; ◑SI = slope indicator; +P = test pit; dashed lines denote sections shown in Figs. 4, 5, and 7; contour interval = 50 ft (15 m).

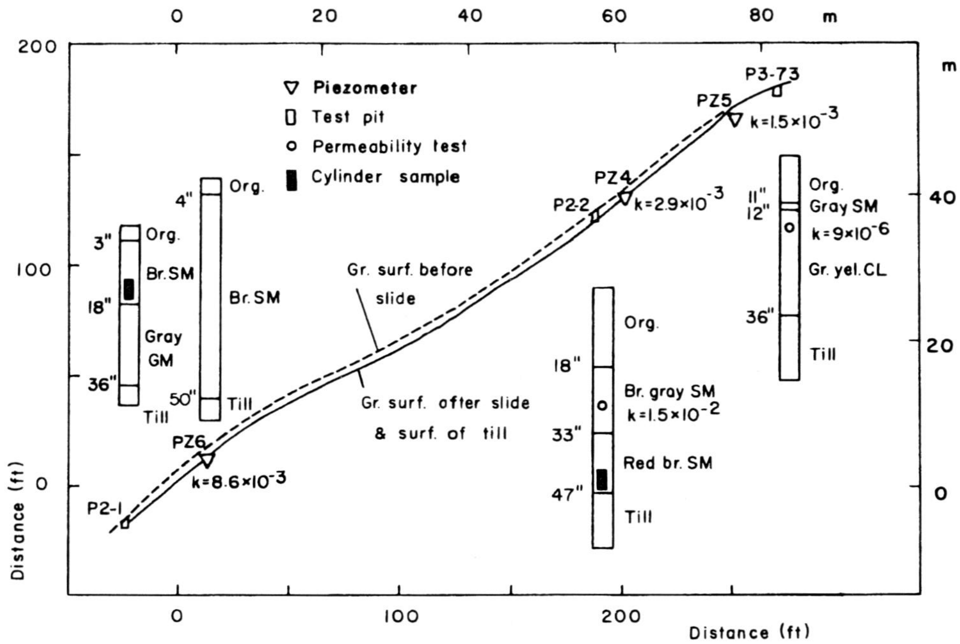

FIG. 4. Section 1 (1 ft = 0.3 m); k in ft/min (1 ft/min = 30 cm/min).

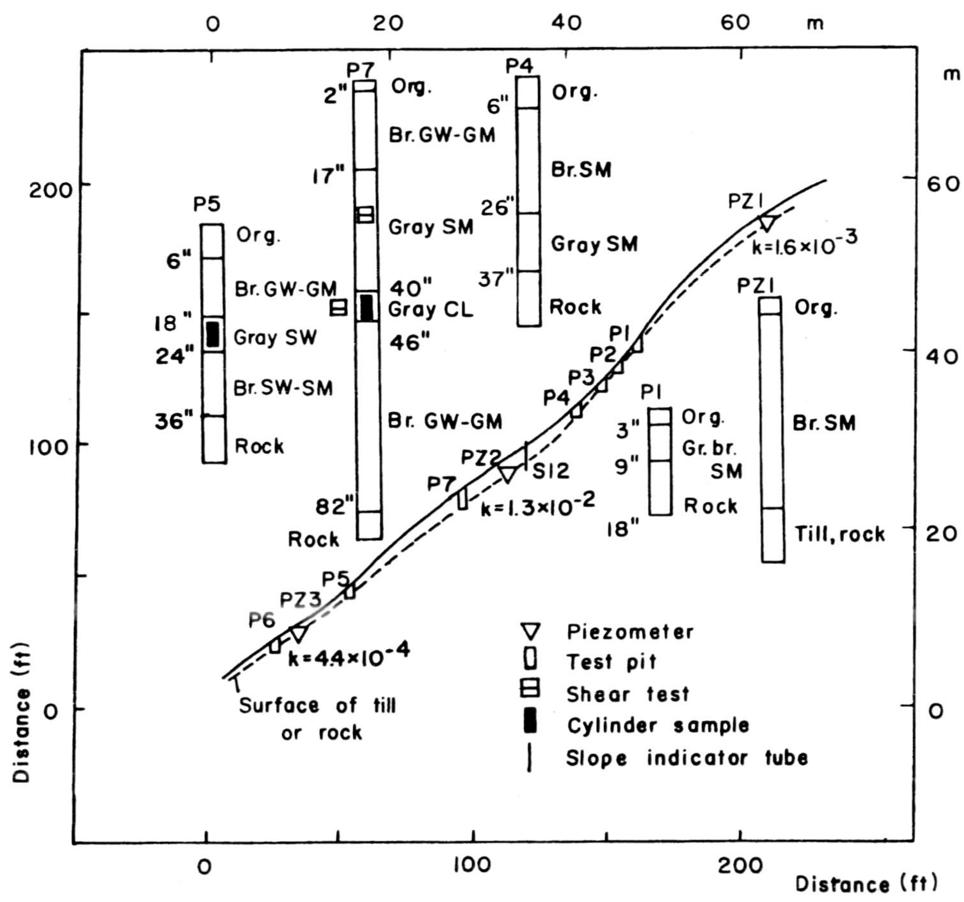

FIG. 6. Small slide on a steep slope in forest. The mass was undermined by slides on the downhill side. Note broken roots.

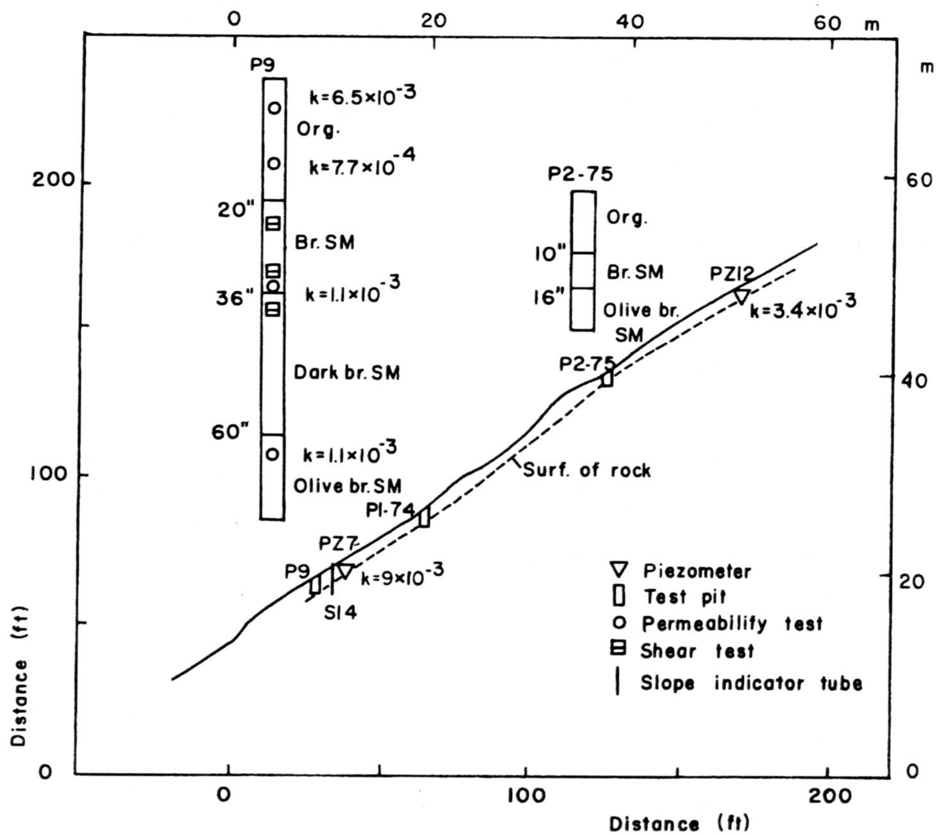

FIG. 7. Section 4 (1 ft = 0.3 m); k in ft/min (1 ft/min = 30 cm/min).

The olive brown silty sand encountered at a depth of 1.5 m (60 in.) is very stiff and gradually changes to estimated that the age of this soil profile is of the order of 400 years (K. R. Everett, personal com-

FIG. 8. Exposed roots.

this area contains many depressions and test pit P2-75, dug in a depression, shows a much thinner weathered zone. Such depressions often occur on the downhill side of large trees the roots of which are exposed, as shown in Fig. 8. Examination of growth rings led to the conclusion that these roots have been exposed to air for at least 60 years (D. R. M. Scott, personal communication, 1975). Thus, it appears that a part of the surface soil has been removed during the last 400 years. However, during recent times at least, the slope has been stable.

The soils in this area have been assigned to the Karta series and the Karta–Tolstoi complex by Gass *et al.*[1] The Karta soil is derived from weathering of till on relatively steep slopes. The soil profiles as revealed in test pits are shown on the cross sections of Figs. 4, 5, and 7. In general, there is a surface layer of organic matter of variable thickness. Below this is the weathered zone (B horizon), which consists of brownish sand and silt with variable amounts of gravel. The gravel content is fairly low in sections 1 and 4 but higher in section 2. Some of the weathered soil in section 2 may be colluvium and may belong to the Tolstoi series (Gass *et al.*[1]). With a few exceptions, most of the soils in the weathered zone are classified as SM or SW in the unified system. In section 1 the material below the weathered zone (C horizon) is predominantly gray glacial till. In sections 2 and 4, the till is often very thin and cannot always be separated from weathered rock. In all of the slides that have been observed, the slip surface lies along the bottom of the weathered soil.

Area B (Fig. 2) was logged by clear-cutting in 1969. A representative section of area B is shown in Fig. 9. The slope is much flatter than those in area A. Soil conditions are generally similar to those in area A. Areas C, D, and E in Fig. 2 indicate slides that occurred between 1971 and 1974. These areas were not instrumented and these slides were not investigated.

Field and Laboratory Investigations

The field and laboratory investigations were carried out to obtain information needed for analysis of slope stability. Figure 10 shows a section of an infinite slope; ab is the slip surface. The forces acting on the element abcd are W_s, the weight of the element abcd; W_t, the weight of the tree(s); F_w, the wind force; and T and N, respectively, the shear and normal components of the reaction force on ab. In addition, we need to know the shear strength of the soil along ab, the contribution of the tree roots to this shear strength, and the piezometric level is represented by h_2 or h_w. Since the slip surface has been observed to lie on the boundary between the weathered and unweathered zones, $h_1 + h_2$ denotes the thickness of the weathered zone. The following sections describe the investigation of soil properties, the strength of the soil–root system, the piezometric level, and the evaluation of the forces F_w and W_t.

Permeability

In situ permeability tests were performed by raising the water level in the standpipe of a piezometer and measuring the rate of discharge. Falling head permeability tests were also performed in test pits. A metal cylinder was pushed into the soil at the bottom of the pit so that its lower end was about 10 cm below the surface of the soil. The cylinder was filled with water and the change in water level with time was measured. Each test was continued until the rate of flow approached a constant value. It is assumed that this represents the permeability of the saturated soil.

The permeabilities were computed from the solutions by Hvorslev (1951) and are shown on the profiles where appropriate (Figs. 4, 5, 7, 9). Most of the measured permeabilities fall between 0.3×10^{-3} and 0.3×10^{-2} m/min (10^{-3} and 10^{-2} ft/min) with the average near 0.6×10^{-3} m/min. There appears to be no significant difference between the ranges of permeabilities measured at the different sections. As a check, the permeability k (cm/s) was estimated

[1]Gass, C. R., Billings, R. F., Stephens, F. R., and Stevens, M. E. Soil management report for the Hollis area. South Tongass National Forest, Ketchikan, AK.

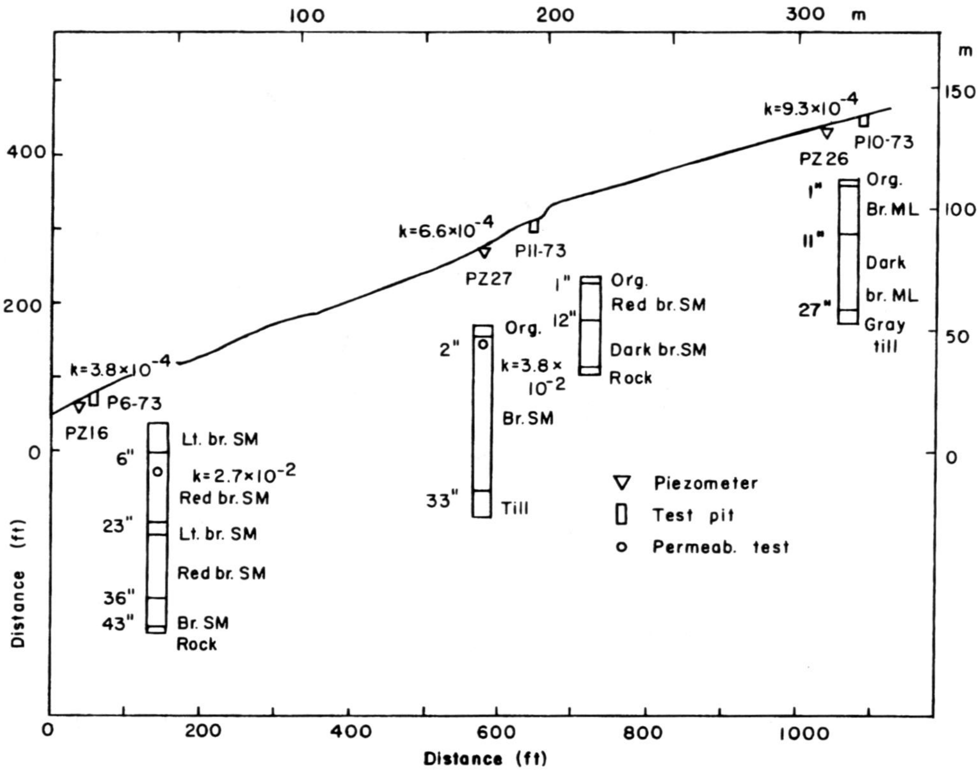

FIG. 9. Section of area B (1 ft = 0.3 m); k in ft/min (1 ft/min = 30 cm/min).

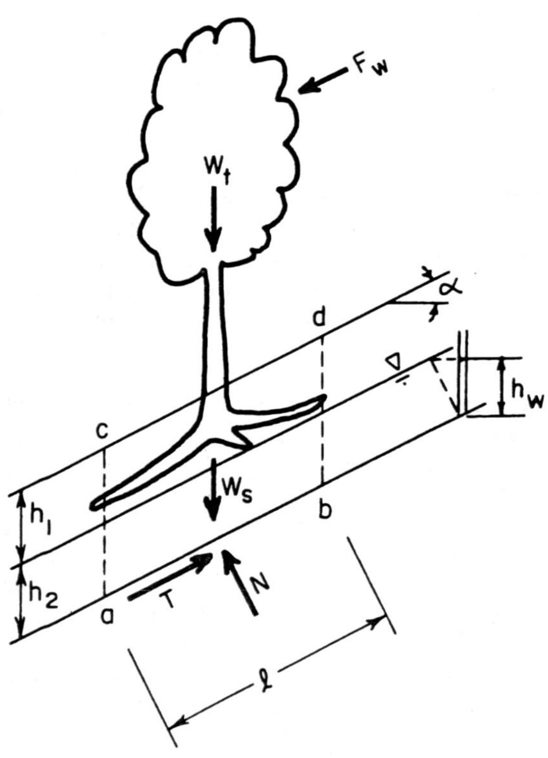

FIG. 10. Forces on sliding soil mass.

from the diameter of the finest 10% of the soil, d_{10} (cm), by means of the equation

$$k = C_1 d_{10}^2 \quad [1]$$

where C_1 ranges between 100 and 150 (Terzaghi and Peck 1967). The computed permeabilities also fall in the above range.

Shear Strength of Soil

From some test pits relatively undisturbed samples were taken by trimming the soil into steel cylinders 15 cm in diameter and 22.5 cm long. The process is similar to that described as 'advanced trimming' by Hvorslev (1949). Drained direct shear tests were performed in the laboratory on these samples. The samples were trimmed to fit into the shear box which measured 6.3 cm square. Samples that contained more gravel were extruded directly into a shear box 15 cm in diameter. Because of the small number of available samples, several tests were performed on each sample. The first test was performed with a normal stress approximately equal to the overburden pressure. This approximates the condition during a dry period. After this the shear box was returned to the initial position and the sample was submerged in

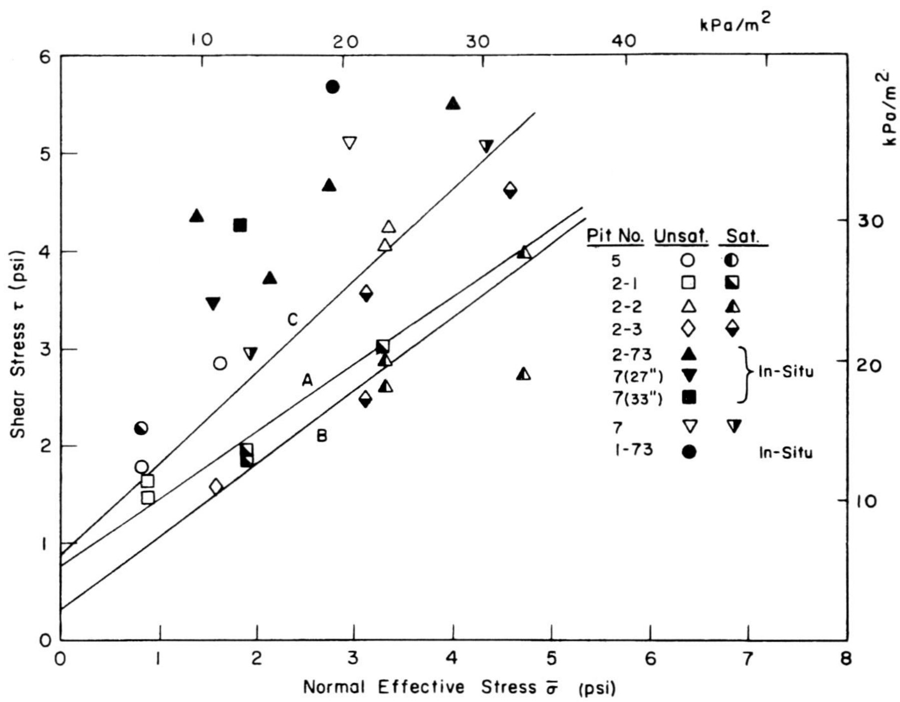

FIG. 11. Results of shear tests (1 psi = 6.9 kPa).

water. The test was repeated. This was followed by tests under higher normal stresses. The results of the shear tests on two samples each from pits 2-1, 2-2, and 2-3 and one each from pits 5 and 7 are shown in Fig. 11. In a few tests on submerged samples the shear was carried out to large displacements to measure the residual shear strength. The residual angle of internal friction is very close to ϕ', the angle of internal friction measured at peak strength. Hence, the shear strength shown in Fig. 11 also represents the residual strength. The results of tests on submerged samples are used as a measure of the strength during the rainy season when the water table rises above the failure surface.

In situ shear tests were performed with a box 30.5 m square. Because it was not feasible to saturate the soil, all tests were made at the *in situ* water content. The results are also shown in Fig. 11. There appears to be some difference between the results of laboratory and *in situ* shear tests on the unsaturateds oils. Because of the large scatter in the data, no conclusions are drawn with regard to the differences.

The wide scatter in the data introduced considerable uncertainty in the choice of the cohesion c' and the angle of internal friction ϕ'. Since the slip surface was below the water table at the time of the slides, the strength in the saturated condition should be used for stability analysis. Hence, the following discussion on shear strength is limited to the data from laboratory tests on saturated samples. The best fit obtained by regression analysis (line A, Fig. 11) gives $c' = 5.3$ kPa (0.75 psi) and $\phi' = 34.7°$. A reasonable estimate of the minimum strength is shown as line B. This gives $c' = 2.1$ kPa (0.30 psi), and $\phi' = 37°$. The minimum strength may be used to estimate the stability of small areas underlain by weak soil. Our estimate of the maximum strength is shown as line C, which gives $c' = 6.0$ kPa (0.85 psi), and $\phi' = 44°$. Use of the maximum strength in stability analysis would indicate whether slides would be widespread or limited to areas of lower strength.

Root Characteristics and Strength

In various test pits, the roots of trees have been observed to extend into the unweathered till and weathered bedrock. They may be expected to contribute to the shear strength of the soil as indicated by the studies of Endo and Tsuruta (1969), Kassif and Lopelovitz (1968), Kaul (1965), and Manbeian (1973). The tensile strengths of roots were measured by the device shown in Fig. 12. The upper end of a root was attached to the calibrated spring. The device was pulled up by hand and the tensile force was determined from the spring compression. A scale attached to the ground surface was used to measure the dis-

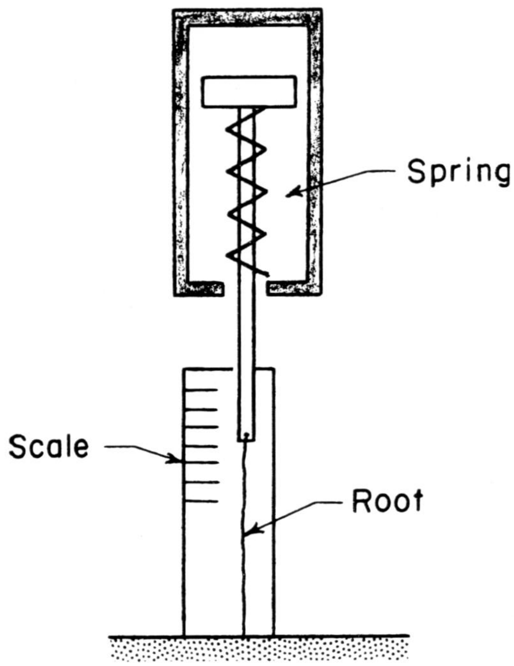

FIG. 12. Device for measurement of root strength.

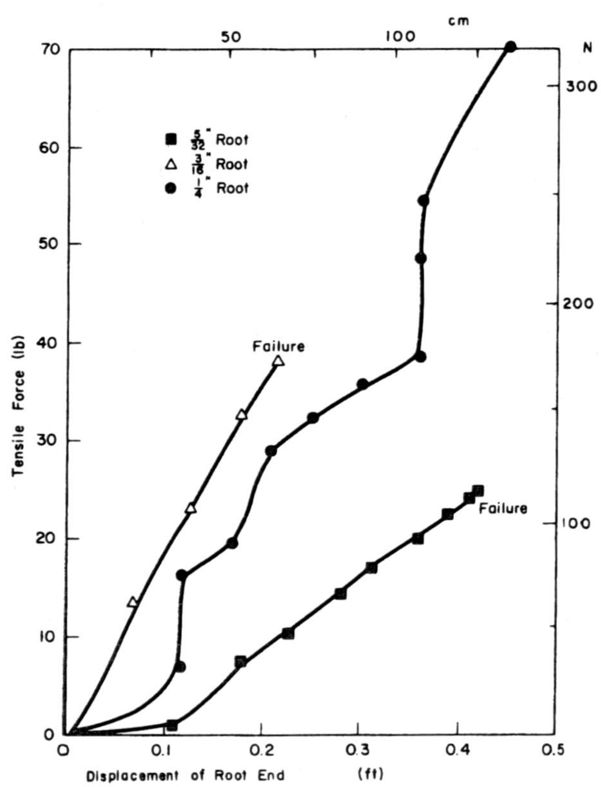

FIG. 13. Load–displacement curves of roots (1 lb = 4.45 N; 1 ft = 30 cm).

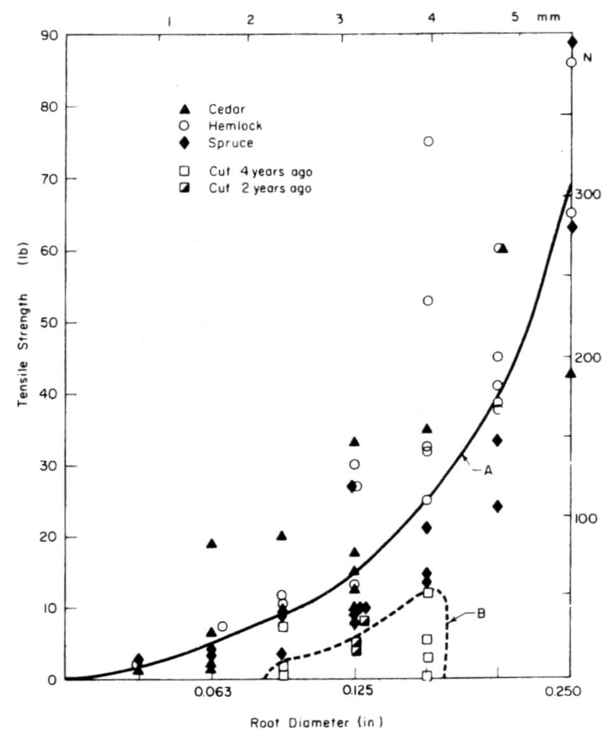

FIG. 14. Relationship between root diameter and failure load (1 lb = 4.45 N; 1 ft = 30 cm).

placement of the end of the root. Typical load versus displacement curves are shown in Fig. 13. Failure occurred by tension failure of the root, or by the root pulling away from the soil, or by a combination of the two.

The ultimate load is plotted against the root diameter in Fig. 14. All the roots tested in area A were located near live trees and it is assumed that curve *A* represents the average strength of live roots. Area B (Fig. 2) was logged in 1969 and the roots tested were located near stumps. Most of the measured strengths fall within the zone indicated as B in Fig. 14. We can see that there is a very marked decrease in root strength after a tree has been cut. Decrease in root strength after the cutting of the tree has also been observed by Burroughs and Thomas (1977), O'Loughlin (1974), and Ziemer and Swanston (1977).

In order to estimate the number of roots present along a slip surface, excavations were made around the roots of several trees. Examination of roots in many test pits indicates that the lateral roots are located mostly in the B horizon, whereas smaller sinker roots grow downwards from a lateral root and extend into the C horizon, which is composed of unweathered till or weathered bedrock (Fig. 15*a*). It has also been observed that when a soil mass fails in shear, the sinker roots are broken (Fig. 6). In a number of excavations the numbers of exposed roots and their diameters were recorded.

Weight of Trees

The numbers of standing trees in four plots in the virgin forest were counted. The four plots are approximately 30 m square and are shown in Fig. 3 with numbers 1–4. The diameters of the trees were also recorded. In addition, the exposed root mats of all downed timber were measured.

The weight of the trees was estimated from the number of trees per unit area and their sizes as determined from the survey. The weight per unit area p_t was obtained by dividing the weight W_t by the area of the root mat. A value of about 5.2 kPa (105 psf) was obtained. Considering the fact that the root mats of live trees may be somewhat greater than those of fallen trees, the above procedure is likely to overestimate p_t. Bishop and Stevens (1964) estimated the average pressure by considering the total weight of trees on a slope to be distributed over the entire area of the slope. They obtained an estimate of 2.5 kPa (50 psf) for p_t.

Strength of Soil–Root System

A number of authors have commented on the effect of roots on slope stability (Bishop and Stevens 1964; Gray 1970; Swanston 1970). Others have measured the shear strengths of soils with roots and compared them with those of soils without roots (Kassif and Lopelovitz 1968; Kaul 1965; Manbeian 1973). In general, the shear strength increases as the number of roots increases.

Figure 15*b* shows the model of the soil–root system subjected to shear. The shear zone is indicated by aa and bb, and θ is the shear distortion. The root, initially in position cd, is moved into position cd′. The tension, T_r, in the root is resolved into components perpendicular and parallel to the shear zone as shown in Fig. 15*b*.

If we let $T_r/A = t_r$, where A = area of a rectangle with sides bb and 1, then

$$[2] \qquad \sigma_r = t_r \cos\theta, \quad \tau_r = t_r \sin\theta$$

where σ_r and τ_r = the normal and shear stresses applied to the soil by T_r. The root's contribution to shear strength is

$$[3] \quad s_r = \sigma_r \tan\phi' + \tau_r = t_r (\cos\theta \tan\phi' + \sin\theta)$$

If we consider all the roots in area A, then

$$[4] \qquad t_r = \Sigma T_{ri}/A$$

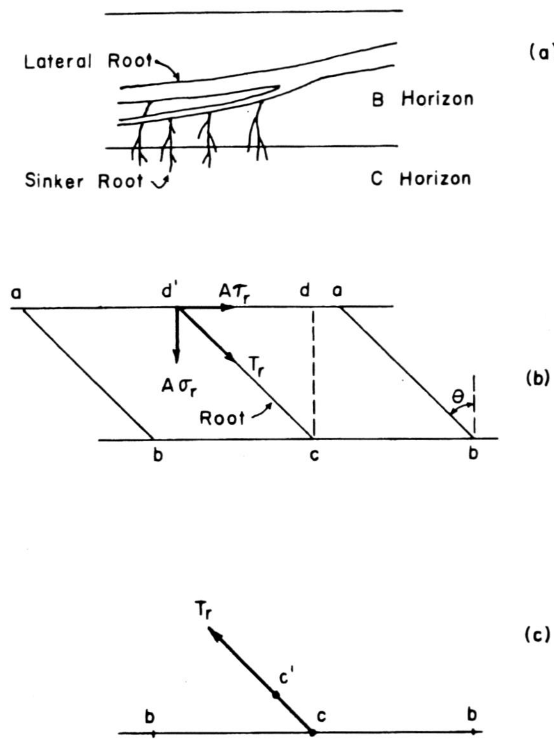

FIG. 15. Strength of soil–root system.

T_r and t_r reach maximum values at failure when T_r is equal to the ultimate load. However, θ at failure is not definitely known. From Fig. 15*b*, it can be seen that the root is extended during shear. Therefore, the value of θ depends on the thickness of the shear zone and the extension of the root at failure. Next, consider the part of the soil below the shear zone. A force T_r would pull the root out of the soil below bb (Fig. 15*c*). Thus point c, initially located on surface bb would move to c′. The situation is similar to the test shown in Fig. 12. We see from Fig. 13 that a displacement of at least 7.5 cm (0.25 ft) is required to produce failure of roots. This means that cc′ should be about 7.5 cm at failure. The same condition holds at the top of the shear zone aa. Thus, the distance cd′ (Fig. 15*b*) would be 15 cm larger than the thickness of the shear zone. The extension of the root within the shear zone is ignored. If the shear zone is 7.5 cm (0.25 ft) thick, then $\theta = 71°$ at failure. If the shear zone is 30 cm (1 ft) thick, $\theta = 48°$. It does not appear likely that the shear zone would be thicker than 30 cm. Hence, θ should be at least 48° and may be as large as 72°. If the extension of the root within the shear zone is included, θ would be still larger, but cannot exceed 90°. This provides an order of magnitude estimate of θ. We note that the gray clay layer in test pit P7 (Fig. 5) is 15 cm (6 in.) thick. If this layer is

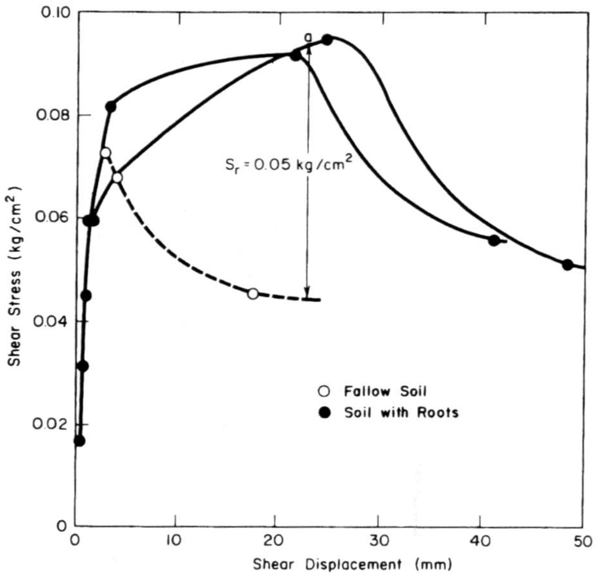

FIG. 16. Stress–displacement curves (after Fig. 4.7 of Manbeian 1973).

taken to be the shear zone, then the above estimates of θ would seem reasonable.

Values of s_r were computed with [3] for different values of θ. The results show that the quantity (cos θ tan ϕ' + sin θ) is insensitive to the value of θ, and is close to 1.2 for the range of θ from 48–72° considered. Hence, we take

[5] $$s_r = 1.2t_r$$

The quantity s_r is nearly constant and would have the characteristics of cohesion.

To estimate the strength of the soil–root system on the slopes in area *A*, the number of roots and the tensile strength of roots as defined by the line A in Fig. 14 were used to calculate t_r by [4]. The results show that t_r lies between 4.2 and 5.5 kPa (87 and 113 psf) and a value of 4.9 kPa (100 psf) is chosen as the average value of t_r. From [5] we get s_r = 5.9 kPa (120 psf). The shear strength of the soil–root system is then given by

[6] $$s^* = s + s_r = c' + \sigma' \tan \phi' + s_r$$

where s = shear strength of the soil, and σ' = effective normal stress.

Analysis of Manbeian's Data

It is desirable to check the validity of [3] against the results of laboratory shear tests on soils with and without roots. The most comprehensive data are those obtained by tests Manbeian performed on soils without roots (fallow soil) and on soils containing roots of various farm crops. Figure 16 shows Manbeian's results. The contribution of the roots is taken as the maximum difference between the shear strengths of the fallow soil and of the soil with roots. In Fig. 16, this is shown as point a and s_r = 4.9 kPa (0.05 kg/cm²). Also, the average tensile strength of the roots is 6.9 kPa. The area of the failure surface is 513 cm². From [4] we obtain t_r = 3.9 kPa.

Manbeian did not perform any pullout tests on his roots. However, consideration of the tensile strain of the roots in the shear zone leads to a value of θ = 45°. This would be the lowest value of θ. If the portions of the roots above and below the shear zone are pulled out, θ would be considerably larger. Calculations with [3] show that s_r would range from 5.0–3.9 kPa for values of θ between 45 and 90°. This range is close to the value of 5.0 kPa estimated from the results of shear tests. From a second test on a soil with barley roots, s_r = 3.6 kPa was obtained. Thus, we see that [3] gives answers that are of the right order of magnitude.

Pore Pressures

The measured piezometric levels for 1965 and 1974 are shown in Figs. 17 and 18, together with the daily precipitation. All of the piezometers had their tips located at the bottom of the weathered zone. Hence, the piezometric heads in these figures are equivalent to h_w, as shown in Fig. 10. We first consider the data for 1965. It has been observed that the piezometric level is highest in piezometers located near the top of the steep part of the slope (near elevation 1300 ft (396 m), Fig. 3). For example, compare the 1965 piezometric levels in piezometers Pz 15, Pz 3S, and Pz 12S (Fig. 17). Similar differences were observed in the 1974 measurements. This trend agrees with the observation that most of the slides initiated near the top of the steep part of the slope.

To assess the pore pressure, one should note that the response of the piezometric level to rainfall is influenced by several factors. The most important factors are the permeability, the relationship between pressure and moisture content, and the rate of water loss by evapotranspiration and drainage. As a simplification we assume that the permeability, the pressure versus moisture relationship, and the drainage of a forested slope are the same as those of a cutover slope. Then any difference in the piezometric response could be attributed to the reduced evapotranspiration in the cutover area. A reduced evapotranspiration would lead to higher piezometric levels.

If we consider the piezometric levels measured in 1974 we note that the water levels in the piezometers located in the cutover area (Pz 13, Pz 14, Pz 15) are

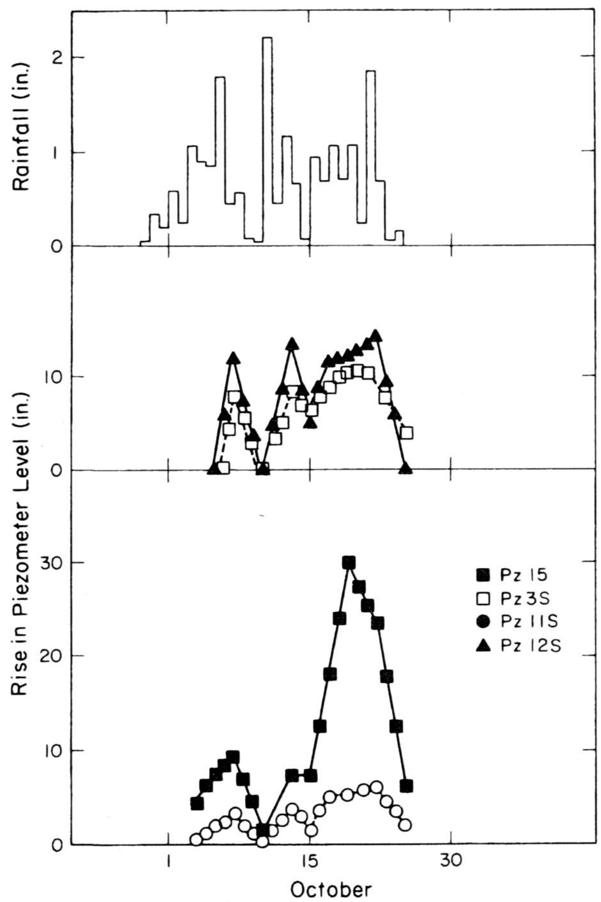

FIG. 17. Piezometric levels, 1965 (1 in. = 2.5 cm).

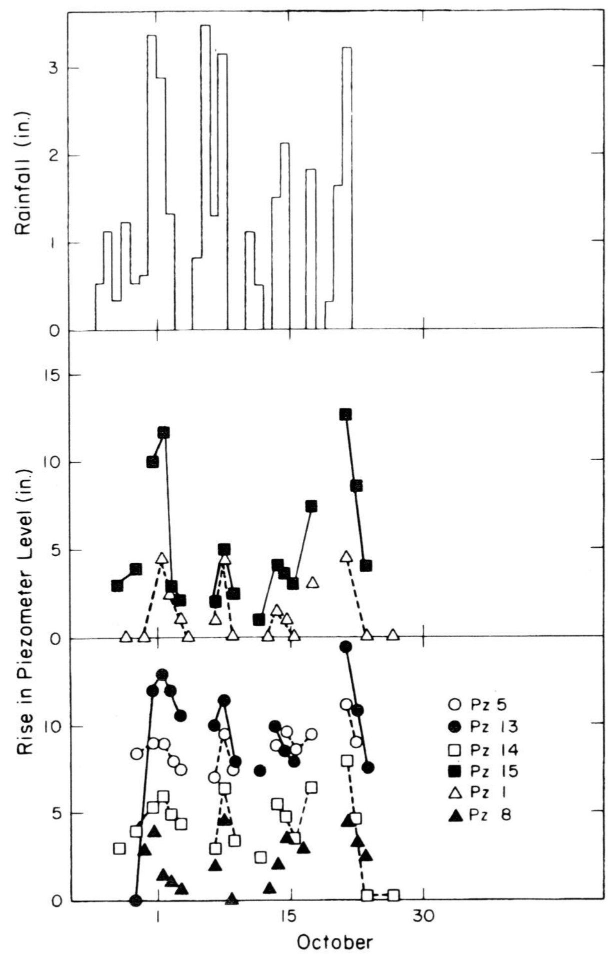

FIG. 18. Piezometric levels, 1974 (1 in. = 2.5 cm).

not higher than those in the forest. This is not surprising as the regrowth was well established in 1974. However, comparison of the piezometric levels of 1974 with those of 1965 shows very significant differences. For example, in piezometer Pz 15, the measured water level in 1965 is much higher than in 1974, although the rainfall intensity for 1965 is considerably lower.

For the purpose of stability analysis, it is necessary to choose the pore pressures for the sections shown in Figs. 4, 5, 7, and 9. The conditions to be investigated are listed in Table 1. For section 1 after logging (case 1) the maximum piezometric level is 76 cm (30 in.) in 1965 (see Fig. 7). To compute h_2 for

TABLE 1. Parameters for stability analysis of slopes

Case	Area or section	$h_1 + h_2$ (in.)	h_w (in.)	α (deg)	P_t (psf)	τ_w (psf)	s_r (psf)	F_s* (a)	F_s* (b)	F_s* (c)	Condition and time
1	1	48	30	39	0	0	20	1.1	0.9	0.6	After clear-cut; 1961–1965
2	1	48	20	39	0	0	20	—	1.0	—	After clear-cut; 1961–1965
3a	2	40	15	50	77	2	120	1.5	1.3	1.0	Virgin forest; 1974
3b	2	40	>15	50	77	2	120	<1.5	<1.3	<1.0	Virgin forest; 1969
3c	4	40	15	35	77	2	120	2.1	1.8	1.6	Virgin forest; 1974
4	3	40	15	40	0	0	0	1.4	1.1	0.8	Virgin forest, no trees; 1974
5	B	30	27	23	0	0	20	2.4	2.0	1.4	After clear-cut; 1974

NOTES: 1 in. = 2.54 cm; 1 psf = 0.05 kPa.
*Columns (a), (b), and (c) list F_s for maximum, average, and minimum shear strengths, respectively.

seepage parallel to the slope (Fig. 10), we use the relationship

$$h_w = h_2 \cos^2 \alpha \qquad [7]$$

where α = angle between the ground surface and the horizontal, and obtain h_2 = 122 cm (48 in.). Thus, the water table is at the ground surface in this case. The slope failure occurred in 1961. Although the rainfall intensity in 1961 was substantially greater than that in 1965, h_2 could not exceed 122 m. Hence, this is considered reasonable for 1961.

Cases 3*a*, 3*b*, and 4 represent, respectively, sections 2, 4, and 3 in the forest. The maximum value of h_w measured in 1974 is between 30 and 38 cm (12 and 15 in.) (Fig. 18). Since the rainfall intensities for 1961 and 1969 are considerably higher than that in 1974, the value of h_w could have been greater than 38 cm in 1961 and 1969. In area *B* (case 5), it was observed that the piezometric level rose to about h_w = 69 cm (27 in.) after heavy rains in October. Hence, h_2 = 76 cm (30 in.) and the entire soil layer is saturated.

Stability Analysis

For an infinite slope with steady seepage (Fig. 10), the safety factor may be expressed as

$$F_s = \frac{S_s + S_r}{T} = \frac{(W_s' + W_t)\cos\alpha \tan\phi' + c'l + s_r l}{(W_s + W_t)\sin\alpha + F_w} \qquad [8]$$

where W_s' = the weight of the soil minus the buoyancy, and S_s and S_r = the shearing resistance of the soil and the roots over the area $l \times 1$. Expressing the forces in terms of unit weights, and taking the width of the column as 1, we have

$$\begin{aligned} W_s' &= \gamma_1 h_1 + (\gamma_2 - \gamma_w)h_2 \\ W_s &= \gamma_1 h_1 + \gamma_2 h_2 \\ W_t &= p_t/\cos\alpha \\ F_w &= \tau_w/\cos\alpha \\ l &= 1/\cos\alpha \end{aligned} \qquad [9]$$

where p_t = the weight of the trees per unit area of the slope, τ_w = the shear stress from the wind, and γ_1, γ_2 = unit weight of the soil above and below the water table, respectively. The nature of the various forces and their effects on stability have been considered by Brown and Sheu (1975) and Gray (1970).

It has been shown that p_t is between 2.5 and 5.2 kPa (50 and 105 psi). An average of 3.8 kPa (77 psf) was used in the stability analysis. Trial calculations have shown that the use of 2.5 or 5.2 kPa would change the computed safety factor by less than 0.05.

If the wind is blowing in the downhill direction, then the force F_w should be added to the driving force. The drag force of wind on trees has been measured in experiments with model forests in a wind tunnel (Hsi and Nath 1970). The shear stress is

$$\tau_w = C(\tfrac{1}{2}\rho u_a^2) \qquad [10]$$

where C = drag coefficient, ρ = mass density of air, and u_a = ambient wind velocity. The measured drag coefficient lies between 0.30 and 0.15 at the edge of the forest and decreases to about 0.01 at large distances from the edge. For a wind velocity of 90 km/h, the value of τ_w according to [10] is about 1 kPa (2 psf) at the edge. The amount is rather small and not likely to exert a strong influence on the stability. The effect of vibrations caused by the oscillating motion of trees is not considered.

For analysis of slope stability the following conditions were used for slopes in area *A*. The average depth of the weathered zone ($h_1 + h_2$) and the slope angle α are given in Table 1. Four cases were analyzed as shown in the table. Case 1 represents section 1, Fig. 3, in 1961. This is considered to represent also the condition of slopes a few years after clear-cutting. Hence, p_t = 0, and τ_w = 0. From Fig. 14 we see that 4 years after clear-cutting the root strength is reduced to about 1/6 of the original value. Hence, s_r should be around 1 kPa (20 psf). The pore pressure corresponds to the highest piezometric level (h_w = 76 cm or 30 in.). Calculations were made with the highest, average, and lowest shear strengths shown in Fig. 11. The computed safety factors are 1.1 or lower, which shows that failure should have occurred. To evaluate the effect of pore pressure on stability in section 1, the value of h_w required to give a safety factor of unity was computed using the average shear strength. It was found that h_w = 51 cm (20 in.) (case 2). Consideration of the measured h_w in Fig. 17 shows that the value of h_w at points well below elevation 1300 ft (396 m) are less than 51 cm (20 in.). This is in general agreement with the observation that failures are limited to the region near elevation 1300 ft (396 m) where porewater pressures are highest.

Case 3*a* represents the steep portion of the slope in section 2, Fig. 5. In an area with trees, p_t = 3.8 kPa (77 psf), τ_w = 1 kPa (2 psf), and s_r = 5.9 kPa (120 psf). The pore pressure corresponds to the highest observed piezometric level (h_w = 38 cm or 15 in.) in 1974. It has a safety factor of 1.0 for the case of minimum strength. Because the rainfall intensity in 1969 is larger than that in 1974, the value of h_w in 1969 could be greater than that observed in 1974. Thus the safety factor in 1969 may be expected to be less (case 3*b*). This is in agreement with the observed signs of movements on the steep part of the slope, and the apparent stability of slopes with angles smaller than 50°. Case 3*c* represents section 5 in the virgin forest. The conditions are the same as those for case 3*a*, except that the slope angle is smaller. The computed safety factor is well above 1 for minimum strength and is in agreement with the observation that the slope is stable.

Small areas in the forest that do not have trees are approximated by the conditions in case 4. This applies to the small slide (section 3, Fig. 3) and the computed safety factor is 1.0 for the average strength. This case also illustrates the contribution of tree roots to the shear strength. Much of the slope in the area between sections 1 and 2 (Fig. 3) has a slope angle close to 40°. Thus, if the tree roots do not contribute to the shear strength, slope failures would be widespread in this area.

Slopes in area *B* after clear-cutting are represented by case 5. The computed safety factor is at least 1.4 and the slopes are currently stable. Hence, in general the computed safety factors are in agreement with the observed behavior of the slopes.

Slope Movements

Measurements of slope movements were made from 1965 to 1966 (Barr and Swanston 1970) in the area of slope indicator tube SI1 (Fig. 3). The measured movements range from 0.12–1.2 cm at the surface over a period of 1 year. Creep movements were limited to the top 0.3 m of the soil. Measurements made in 1974 indicate that on stable slopes (sections 1 and 4, Fig. 3) the movements are less than 2.5 cm/year. Measurements in slope indicator tube SI2, located in the unstable area of section 2 (Fig. 5), have shown surface movements as large as 25 cm/year.

Summary and Conclusions

In this investigation of slope failures in shallow surface soils, porewater pressures were measured and the soil properties were evaluated by laboratory and *in situ* tests. A model was developed to describe the shear strength of the soil–root system. The model indicates that the contribution of tree roots to shear strength may be treated as a cohesion. For the roots studied in this area, this cohesion, denoted by s_r, is around 5.9 kPa.

Slope failures in this region frequently occur during periods of heavy autumn rains a few years after the trees have been removed by clear-cutting. Results of stability analyses of representative slopes show that if $s_r = 0$ the slopes are not stable. Stable forested slopes were also analyzed with $s_r = 5.9$ kPa and safety factors substantially greater than 1 were obtained. Thus the results indicate that strength contributed by tree roots is important to the stability of the steeper slopes. Loss of root strength following clear-cutting can seriously affect slope stability.

Acknowledgments

This investigation was supported by grants from the National Science Foundation and the Forest Sciences Laboratory, U.S.D.A. Forest Service, Corvallis, Oregon. The South Tongass National Forest assisted in the logistics for field work. We are grateful to K. R. Everett, C. R. Gass, and D. R. M. Scott for their contributions to the study. The field and laboratory work were carried out with the help of R. A. DeStephen, S. M. Gale, J. B. Givens, D. Huntley, S. S. Lin, and G. B. Shearer.

Barr, D. J., and Swanston, D. N. 1970. Measurement of creep in a shallow, slide-prone till soil. American Journal of Science, **269**, pp. 467–480.

Bishop, D. M., and Stevens, M. E. 1964. Landslides on logged areas in southeast Alaska. United States Department of Agriculture, Forest Service, Northern Forest Experiment Station, Juneau, AK, Research Paper NOR-1.

Brown, C. B., and Sheu, M. S. 1975. Effects of deforestation on slopes. ASCE Journal of the Geotechnical Engineering Division, **101**(GT2), pp. 147–166.

Burroughs, E. R., and Thomas, B. R. 1977. Declining root strength in Douglas-fir after felling as a factor in slope stability. United States Department of Agriculture, Forest Service, Intermountain Forest and Range Experiment Station, Ogden, UT, Research Paper INT-190.

Endo, T., and Tsuruta, T. 1969. The effect of tree roots upon the shearing strength of soil. Hokkaido Branch, Tokyo Forest Experiment Station, Sapporo, Japan, Annual Report No. 18. (In Japanese.)

Gray, D. H. 1970. Effects of forest clear-cutting on the stability of natural slopes. Bulletin of the Association of Engineering Geologists, **7**(1, 2), pp. 45–66.

Hsi, G., and Nath, J. H. 1970. Wind drag within a simulated forest. Journal of Applied Meteorology, **9**(4), pp. 592–602.

Hvorslev, M. J. 1949. Subsurface exploration and sampling of soils for civil engineering purposes. American Society of Civil Engineers, New York, NY.

——— 1951. Time lag and soil permeability in groundwater observations. Waterways Experiment Station, Corps of Engineers, Vicksburg, MI, Bulletin No. 36.

Kassif, G., and Lopelovitz, A. 1968. Strength properties of soil root systems. Soil and Roads Lab, Faculty of Civil Engineering, Technion-Israel Institute of Technology, Haifa, Israel.

Kaul, R. 1965. The influence of roots on certain mechanical properties of an uncompacted soil. Ph.D. thesis, Department of Agricultural Engineering, North Carolina State University, Raleigh, NC.

Manbeian, T. 1973. The influence of soil moisture suction, cyclic wetting and drying, and plant roots on the shear strength of cohesive soil. Ph.D. thesis, Department of Soil Science, University of California, Berkeley, CA.

O'Loughlin, C. L. 1974. A study of tree root strength deterioration following clearfelling. Canadian Journal of Forest Research, **4**, pp. 107–113.

Swanston, D. N. 1967. Soil-water piezometry in a southeast Alaska landslide area. United States Department of Agriculture, Forest Service, Pacific Northwest Forest and Range Experiment Station, Portland, OR, Research Note PNW-68.

——— 1969. Mass wasting in coastal Alaska. United States Department of Agriculture, Forest Service, Institute of Northern Forestry, Juneau, AK, Research Paper PNW-83.

——— 1970. Mechanics of debris avalanching in shallow till soils of southeast Alaska. United States Department of Agriculture, Forest Service, Institute of Northern Forestry, Juneau, AK, Research Paper PNW-103.

Terzaghi, K., and Peck, R. B. 1967. Soil mechanics in engineering practice. John Wiley and Sons, New York, NY.

Varnes, D. J. 1958. Landslide types and processes. *In* Landslides and engineering practice. *Edited by* E. B. Eckel. Highway Research Board, Special Report 29, pp. 20–47.

Ziemer, R. R., and Swanston, D. N. 1977. Root strength changes after logging in southeast Alaska. United States Department of Agriculture, Forest Service, Pacific Northwest Forest and Range Experiment Station, Portland, OR, Research Note PNW-306.

Notation

c' = cohesion
d_{10} = diameter of the finest 10% of the soil
h_1 = vertical distance from ground surface to water table
h_2 = vertical distance from water table to slip surface
h_w = piezometric head
k = permeability
l = length of slip surface
P_t = weight of trees per unit area
s = shear strength of soil
s_r = contribution of roots to shear strength
t_r = tensile stress in root
u_a = wind velocity
A = area
C = constant coefficient
F_s = safety factor
F_w = wind force
N = normal component of reaction on slip surface
S = shearing resistance
T = shear component of reaction on slip surface
T_r = tensile force in root
W_s = weight of soil
W_s' = weight of soil minus buoyancy
W_t = weight of tree(s)
α = slope angle
γ = unit weight
θ = shear distortion
ρ = mass density
σ = normal stress
τ = shear stress
τ_w = shear stress due to wind
ϕ' = angle of internal friction